Available online at www.sciencedirect.com
ScienceDirect
Proceedings of the Combustion Institute 31 (2007) 2157–2164
Proceedings of the Combustion Institute
www.elsevier.com/locate/proci

Experimental study of the effect of helium/nitrogen concentration and initial droplet diameter on nonane droplet combustion with minimal convection

J.H. Bae [1], C.T. Avedisian *

Sibley School of Mechanical and Aerospace Engineering, Cornell University, Ithaca, NY 14853-7501, USA

Abstract

In this paper, we study the influence of inert concentration and initial droplet diameter on nonane (C_9H_{20}) droplet combustion in an environment that promotes spherical droplet flames. The oxygen concentration is fixed while the inert is varied between nitrogen and helium. A range of initial droplet diameters (D_o) are examined in each ambient gas: 0.4 mm $< D_o <$ 0.8 mm; and an oxidizing ambiance consisting of 30% oxygen (fixed) and 70% inert (fixed), with the inert in turn composed of mixtures of nitrogen and helium in concentrations of 0, 25, 50, 75, and 100% N_2. The experiments are carried out at normal atmospheric pressure in a cold ambiance (room temperature) under low gravity to minimize the influence of convection and promote spherical droplet flames. For burning within a helium inert (0% N_2), the droplet flames are entirely blue and there is no influence of initial droplet diameter on the local burning rate (K). With increasing dilution by nitrogen, droplet flames show significant yellow luminosity indicating the presence of soot and the individual burning histories show K reducing with increasing D_o. The evolution of droplet diameter $D(t)$ is nonlinear for a given D_o in the presence of either helium or nitrogen inerts indicating that soot formation has little to do with nonlinear burning. A correlation is presented of the data in the form $(D/D_o)^{2(1+\varepsilon)} = 1 - K't/D_o^{2(1+\varepsilon)}$ where the effective burning rate, K', and ε are concentration-dependent. Correlations for these parameters are presented in the paper.

Keywords: Droplet combustion; Spherical symmetry; Soot formation; Inert concentration; Helium

1. Introduction

The quasi-steady theory of spherically symmetric droplet burning [1–3] was originally developed based on a set of assumptions that led to the so-called "D^2-law". It did not include soot formation or radiation. From this theory the droplet burning rate, $K = -\frac{d(D^2)}{dt}$, where D and t are the instantaneous droplet diameter and time, respectively, is predicted to be independent of the initial droplet diameter, D_o. Experiment and analysis for spherically symmetric droplet burning show trends that conflict with this result [4,5]. In particular, for droplets with D_o under about 1 mm in a cold ambiance, K decreases as D_o increases. Though

* Corresponding author. Fax: +1 607 255 1222.
E-mail address: cta2@cornell.edu (C.T. Avedisian).
[1] Present address: Texas Instruments Incorporated, Sensors and Controls, 529 Pleasant St., MS B-39, Attleboro, MA 02703, USA.

1540-7489/$ - see front matter © 2006 The Combustion Institute. Published by Elsevier Inc. All rights reserved.
doi:10.1016/j.proci.2006.08.042

later independently verified [6], the role of soot formation in this trend has yet to be conclusively explained. Interestingly, in a high temperature gas the opposite trend in the relationship between K and D_o is observed, namely that K increases as D_o increases. This reversal from combustion in a cold gas was explained [7] based on a net heat gain to the droplet in a high temperature ambiance associated with the flame diameter increasing with increasing D_o, as compared to combustion in a cold gas where there is a net heat loss to the droplet with increasing D_o and a lowering of the burning rate.

The objective of this study is to examine the role of the initial droplet diameter and inert gas composition on droplet combustion dynamics in a cold ambient gas for the spherical droplet flame configuration. This is done by comparing the burning process for combustion in an ambiance where soot formation is significant to one where soot formation is reduced considerably, and in each ambiance selected we vary the initial droplet diameter over a controlled range. With all other parameters fixed (e.g., gas temperature, pressure, and fuel type) comparing the results in this way establishes soot's role on the droplet combustion dynamics. The spherical flame is selected for the simple one-dimensional gas transport process it provides. Models developed for the complexities inherent with soot formation will first make this simple assumption and data such as reported here will be useful for modeling.

Nonane (C_9H_{20}) is selected as a model fuel because it is strongly sooting in air, and it has a low propensity for water absorption so that this effect on burning will not be operative [5]. We have previous experience with nonane [8,9], and it is representative of a constituent that is being considered in a model surrogate transportation fuel [10]. Spherical gas phase symmetry in the burning process is realized by a combination of restricting droplet motion, by using 'small' droplets, and by carrying out the experiments in a gravitational field that is low enough so that the effect of convection is reduced.

The experiments are carried out in an oxidizing ambiance with a composition that is varied to control sooting (e.g., through the variation of flame temperature on gas composition). To keep the problem tractable, we fix the oxygen to inert ratio in the gas and vary the inert portion between extremes that will alternately promote and eliminate soot formation, as evidenced by flame structure transitioning from highly luminous (yellow) to blue. We selected a composition of 0.30 oxygen (volume fraction) and then varied the remaining 0.70 inert between nitrogen and helium in increments of 1.0, 0.75, 0.50, 0.25, and 0.0. This corresponds to a total nitrogen inert in the oxygen/inert mixture of 0.70, 0.53, 0.35, 0.17, and 0.0, respectively, to give an ambiance of oxygen/helium/nitrogen.

In each ambient gas composition selected, the initial droplet diameter is varied between 0.4 mm and 0.8 mm, which is a large enough range that the initial diameter would be expected to play a role. The initial droplet diameter range selected is based on our capabilities to observe the complete burning history for the available experimental time and to optically resolve the droplets for a large fraction of its burning history.

The decision to fix the oxidizer concentration and vary the inert composition is a convenient way to control the sooting behavior. The particular choice of a 0.30 oxygen concentration is dictated by our ability to ignite the test droplets for the whole range of inert concentration examined. Helium is a good choice for varying soot formation because of the strong influence it has on the flame temperature and heat transfer to the droplet (due to helium's comparatively high gas thermal conductivity).

Quantitative data are reported on the evolution of droplet, flame and soot shell diameter for all of the conditions examined. These data are used to assess soot formation and to illustrate the extent of unsteadiness of the burning process. Qualitative observations based on color film analysis are included to illustrate the flame structure and flame luminosity that is indicative of soot formation. Also included is development of a correlation for the evolution of droplet diameter that seeks to capture the effect of initial droplet diameter and gas composition by consolidating the data for each gas composition onto a single curve. This is accomplished by ad hoc modification of the classical D^2-law in which the exponent on droplet diameter and effective burning rate are made dependent on inert concentration.

2. Experiment and procedures

The experiments are conducted in a free-fall platform to reduce gravity and buoyancy effects. The free-fall platform is equipped with a drag shield to produce effective gravity levels in the moving frame of reference of about 10^{-4} of Earth's normal gravity [8,9,11]. By using 'small' droplets (range between 0.4 mm to 0.8 mm) and carrying out the experiments under these low gravity conditions, the influence of buoyancy is reduced considerably as measured by the sphericity of the flames; the Rayleigh number is on the order of 10^{-5} to 10^{-6} at 1 atm based on the droplet diameter [8]. During the downward flight of the instrumentation package, the droplet is ignited and the ignition source is withdrawn to provide an unobstructed ambiance for the combustion process, which is recorded by high speed (color, and black and white) 16 mm cine and video photography. The droplets are contained in a chamber with four optical windows that is filled with the gas mixture of interest.

Photographic visualizations provide the information from which quantitative data of droplet, flame and soot shell diameter are extracted. Two cameras are used to view the droplet at 90°. A 16-mm LOCAM II camera operating at 200 frames per second and a shutter speed of 1/450 s with backlighting records droplet and soot shell shape (and diameter). For backlit black and white high-speed imaging, the film used is Kodak #7278 black and white film (ASA 125) and backlighting is provided by a 12-W halogen lamp. Individual movie frames are digitized by a scanner at high resolution and droplet and soot shell diameters are analyzed by Image Pro-Plus 4.0 on a PC with a resolution of 0.5 to 2.5% for droplet diameter. The uncertainty of the measurements is about the size of the symbols displayed in the figures. Without backlighting, a Hitachi HV-C20 CCD video camera with a Nikon 135-mm f2.0 lens and 72-mm extension tube records the flame structure and color, and its variation with helium dilution.

To charge the chamber with the desired gas mixture, the chamber is first put under a vacuum of 76 torr. The ambient gas mixture of interest, stored in pre-prepared bottles (<1% uncertainty), is then introduced into the chamber to flush out the residual air for 60 s and to bring the pressure back to atmospheric with the gas composition of interest. Although it is conceivable that there is some residual of combustion products remaining inside the chamber after this purge, we assumed that any residual would exert a negligible influence because of the small ratio of droplet to total volume: the ratio of droplet to chamber volume is less than 10^{-8}.

Droplets are anchored by two SiC fibers (of 12 μm in diameter) crossed at an angle of 60° and mounted on support stands. Previous work [11] showed that free nonane droplets had virtually identical burning histories to droplets anchored by these very small SiC fibers for the initial droplet diameters that cover the range reported in the present paper. This was demonstrated by comparing the evolution of droplet diameters for free and fiber-supported droplets. The consistency between the two deployment techniques indicates that the comparatively small SiC fibers do not influence the burning rate for the vast majority of the burning process. Similarly, their influence on the flame structure and cooling of the flame is small because of the fiber's very small cross-sectional area for energy flow compared to the overall surface area of the flame.

Droplets could not be manually placed on the fiber because of the small fiber diameter. Instead, we used a piezoelectric drop generator to propel a small droplet to the fiber intersection where it collides with and sticks to the fiber. The specific initial droplet diameter of interest is then created by impinging several droplets on the fiber and building up the size of interest by successive coalescences of the droplet. The package is quickly released into the freefall after deployment.

During the freefall, the droplet is ignited by hot wires from two circular Kanthal A-1 (33 AWG) wires fashioned into 0.5 mm (I.D.) loops. The two loops are positioned horizontally on opposite sides of the droplet to reduce ignition asymmetries at a location close enough that ignition will occur (i.e., from 0.50 to 1 mm from the droplet surface). Electrical power (57 W) to the Kanthal wires is initiated 200 ms after the drop package is released (delay time) and power to the wire loops is kept on for about 200 ms (±30). This delay time allows vibrations to dampen in the instrumentation package caused by the physical separation of the package from the electromagnet which holds the package in place. After ignition the hot wires are quickly retracted (within 10 ms) to allow burning in an unobstructed ambiance. A constant electrical power, as well as accurate shape and placement of the hot wire loops relative to the droplet, are important for reliable and repeatable ignition. Further details of how this was done are given in reference [8].

3. Discussion

Figures 1 and 2 illustrate the soot and flame structure of nonane flames. Figure 1 shows selected backlit photographs and Fig. 2 shows selected color print images. Shown are extremes (most intense images) of the influence of the ambiance, 100% nitrogen or 100% helium. The soot is clearly visible as a shell structure in Fig. 1a that is concentric with the droplet. Figure 1b shows the effect of replacing nitrogen by helium in the 70% inert and it is seen that virtually no soot is visible. In the motion picture sequences, not shown here, there is a gradual transition from Figs. 1a to b. Figure 2 shows flame-illuminated color images with

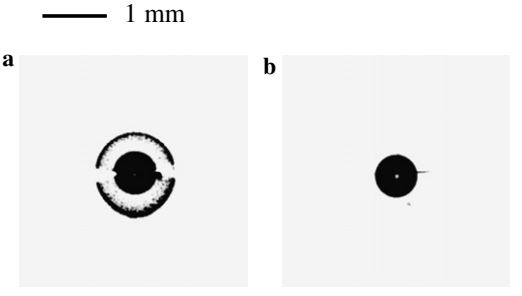

Fig. 1. Backlit photographs taken 150 ms after ignition of nonane droplets with $D_o \sim 0.73$ mm burning in (a) 30% oxygen/70% nitrogen showing droplet and soot shell; and (b) 30% oxygen/70% helium showing only the droplet.

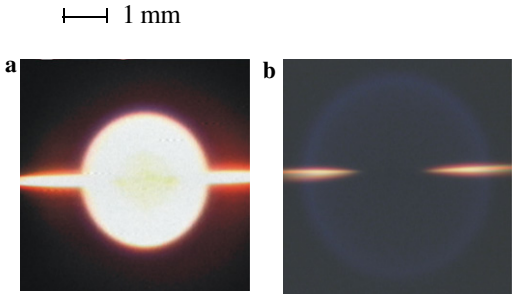

Fig. 2. Flame-illuminated photographs taken 230 ms after ignition of nonane droplets with $D_o \sim 0.73$ mm burning in (a) 30% oxygen/70% nitrogen, and (b) 30% oxygen/70% helium.

Fig. 2a being for a 100% nitrogen droplet flame and Fig. 2b for a 100% helium droplet flame. Again, the images transition from Figs. 2a to b as nitrogen is diluted by helium. At 100% helium (Fig. 2b), the flame is almost entirely blue signifying no soot. The reduction of soot formation for the helium inert is due to the lower flame temperature compared to nitrogen. Quantitative measurements of droplet diameter come from images like that shown in Fig. 1, and flame dimensions come from images like those shown in Fig. 2.

Figures 3a–d show the burning process presented in the coordinates of the D^2-law,

$$\left(\frac{D}{D_o}\right)^2 = 1 - K\frac{t}{D_o^2} \tag{1}$$

(in Figs. 3e to h, modified coordinates are discussed later). Measurements right after ignition are not made because the flame luminosity at high oxygen concentration obscures the droplet. For 100% nitrogen (i.e., 30% oxygen/70% nitrogen) in Fig. 3d, the droplet diameter progressions are quite segregated with larger droplets burning more slowly than smaller droplets. With increasing dilution by helium (Figs. 3c to a), the influence of initial droplet diameter diminishes. This trend clearly shows the effect of both soot formation and initial diameter on burning. Speculations for soot's role have been offered [4,6,12], including heat release at the flame and radiative losses which appear to be connected with the residence time of soot. Nonetheless, quantitative explanation of these trends has not yet been developed.

Close examination of Figs. 3a–d indicates some curvature and unsteadiness to the evolution of droplet diameter, which also means that the burning rate (i.e., rate of change of D^2) exhibits a time dependence. As the droplet disappears it burns faster. This unsteadiness exists even with 100% helium dilution. From this we conclude that soot formation does not influence the time dependency of the burning rate. We believe that a time-dependent burning rate is evidence of droplet heating that persists for the entire period of burning even for these small droplets, caused by a continually increasing droplet temperature and reduction of liquid density even after an initial droplet heating period [13]. Predictions of the droplet temperature [14] show that the droplet heating rate is high immediately after ignition and more gradual thereafter as the droplet temperature asymptotically approaches the wet bulb temperature of the fuel and the heating rate approaches zero. This process can persist throughout burning.

Figure 4 shows the influence of initial droplet diameter and inert concentration on the flame and soot standoff ratio. For 100% helium, data are not shown because the soot shell does not form. As for the soot standoff ratio, D_s/D, it does not show any appreciable influence of inert concentration or initial droplet diameter in the range of 0.4 mm to 0.8 mm which is examined in the present study. On the other hand, the data in Figs. 4a–c suggest that when soot formation decreases, which is brought about by reducing the initial droplet diameter in our experiments for a given gas concentration, the flame moves away from the droplet. We think that for burning in a cold ambiance, that since reducing D_o reduces soot formation, radiation losses from the flame may also be lowered. The flame would then to positioned farther out from the droplet. This speculation is consistent with the data shown in Fig. 4.

4. Correlation of droplet diameter data

As noted previously, the classical theory of droplet burning predicts that the burning rate is independent of D_o. When presented in a plot of $(D/D_o)^2$ vs. t/D_o^2 the data should fall on a single curve independent of D_o. This is clearly not the case for our data as shown in Figs. 3a–d, especially at low helium concentration. The burning process is considerably more complex than the basic theory can account for. As a result, we cannot use the classical formulation for burning (Eq. (1)) without modification to predict our data. Here, K is both time and D_o dependent (as also shown by many previously reported data including those presented in this paper). This motivates a more empirical approach to prediction.

We use Eq. (1) in an ad hoc form to develop a correlation of the data. A generalization of Eq. (1) is suggested from previous work [15–18] in the form

$$\left(\frac{D}{D_o}\right)^n = 1 - K'\frac{t}{D_o^n} \tag{2}$$

As defined in Eq. (2), K' is an 'effective' burning rate with a variable unit, mm^n/s when D and D_o are expressed in millimeters and n as an empirical

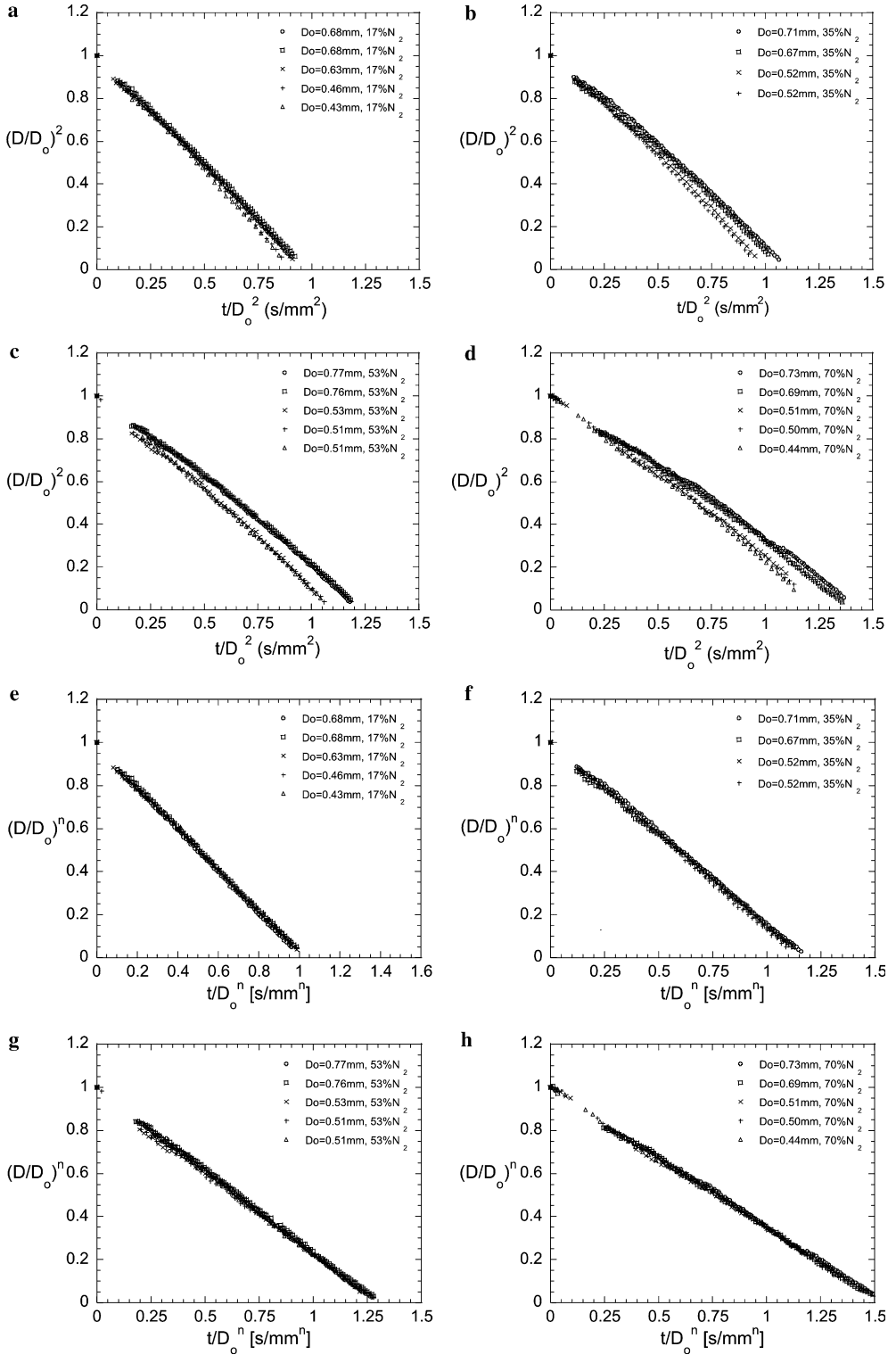

Fig. 3. (a–d) Evolution of droplet diameter presented in traditional D^2 coordinates, Eq. (1); (e–h) evolution of droplet diameter presented in modified coordinates, with exponent 'n' defined by Eq. (2) and determined from data of (a–d) to provide the best fit. Inert is indicated in the inset to the figures.

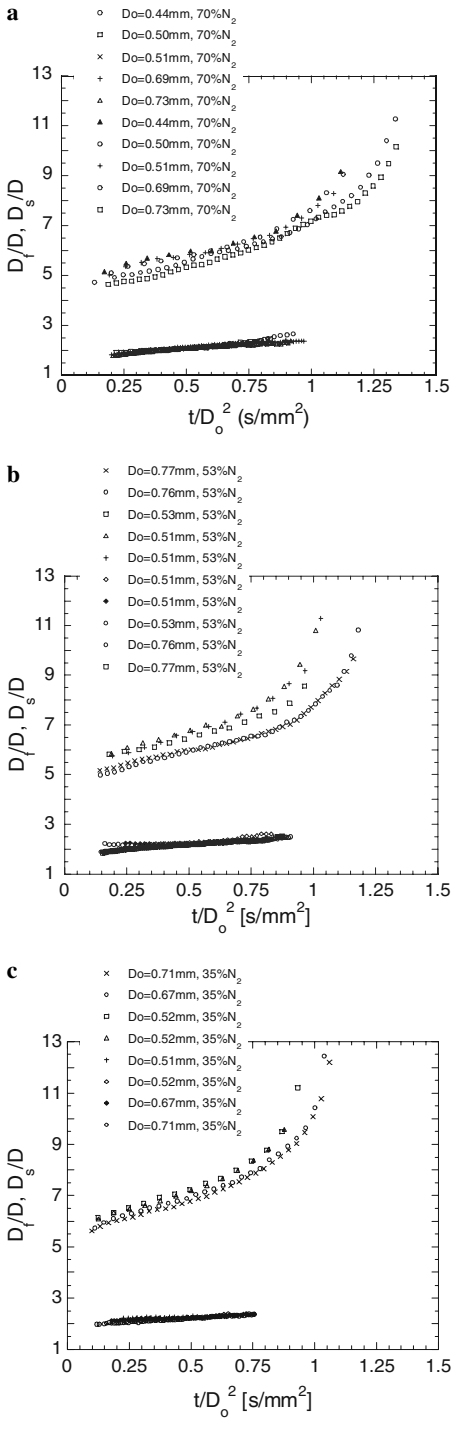

Fig. 4. Evolution of flame and soot standoff ratios showing influence of gas composition and initial droplet diameter: (a) 100% nitrogen inert (30% oxygen/70% nitrogen); (b) 75% nitrogen inert (30% oxygen/53% nitrogen/17% helium); (c) 50% nitrogen inert (30% oxygen/35% nitrogen/35% helium).

value. Equation (2) works for several situations not covered by the D^2 law. For example, monopropellant droplets show that $1 \leqslant n \leqslant 2$ [16,17]; for burning of solid fuels, $n = 3$ [17]; for strong convection $n = 3/2$, and for burning in turbulent flow $n = 1$ [18].

To make the deviation from the D^2-law in Eq. (2) clearer, we write $n = 2(1 + \varepsilon)$ where ε is like a 'correction' factor to the classical law,

$$\left(\frac{D}{D_o}\right)^{2(1+\varepsilon)} = 1 - K'(\phi)\frac{t}{D_o^{2(1+\varepsilon)}} \tag{3}$$

The assumption inherent in Eq. (3) is that the effective burning rate, K', which is indicated as being a function of the volume fraction of nitrogen (ϕ) in the coordinates of $(\frac{D}{D_o})^{2(1+\varepsilon)}$ and $\frac{t}{D_o^{2(1+\varepsilon)}}$, will then be independent initial droplet diameter. However, we should expect a $K'(\phi)$ relationship to account for the influence of gas composition. For added flexibility we have also taken ε to be dependent on gas composition, namely $\varepsilon(\phi)$.

Figures 3e to h display the data of Figs. 3a to d in these new scaled coordinates, with a value of ε that best collapses the data. For all of our measurements, K' is essentially independent of time and does not depend on D_o as shown in Figs. 3e–h. Figures 5 and 6 show the variation of K′ and ε with ϕ that consolidates the data shown in Figs. 3e to h for D and D_o in millimeters. The data are correlated with simple polynomial expressions,

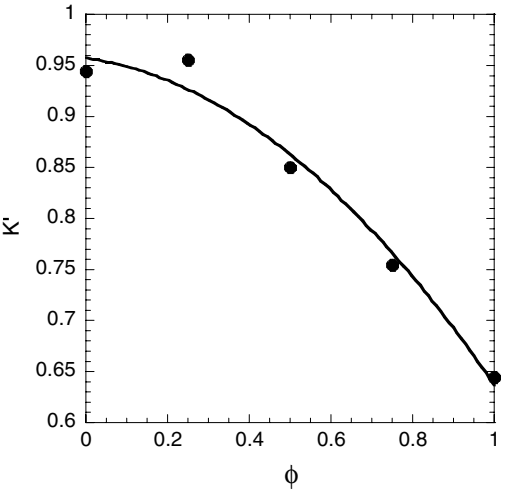

Fig. 5. Variation of effective burning rate as the derivative of the data in Figs. 3e to h with volume fraction of nitrogen (ϕ). The 'unit' of the burning rate is determined by the parameter ε as $mm^{2(1+\varepsilon)}/s$ to be consistent with Eq. (3).

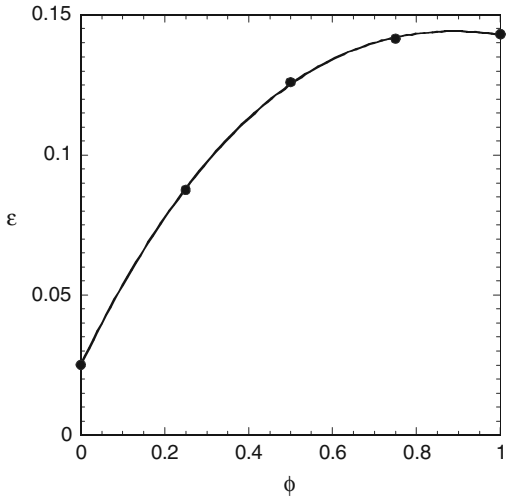

Fig. 6. Variation of ε (Eq. (3)) with volume fraction of nitrogen which collapses the data in Figs. 3a–d.

$$\varepsilon = -0.024886 + 0.3104\phi - 0.2457\phi^2 + 0.533\phi^3 \tag{4}$$

and

$$K' = 0.9574 - 0.0575\phi - 0.2632\phi^2 \tag{5}$$

To illustrate one (of many) comparisons that can be made of Eqs. (3)–(5) with data, Fig. 7 shows the prediction of Eqs. (3)–(5) with the data of Fig. 3c presented in the coordinates of Eq. (1). The comparisons show that the variation of K with D_o and the slight time dependence of K (vs. K') is captured by Eqs. (3)–(5). The restrictions on Eqs. (4) and (5) are that they apply to nonane in the D_o range of 0.4 mm to about 0.8 mm and that the gas concentration is comprised of a fixed oxygen concentration of 30% with the remaining 70% inert being a mixture of helium and nitrogen.

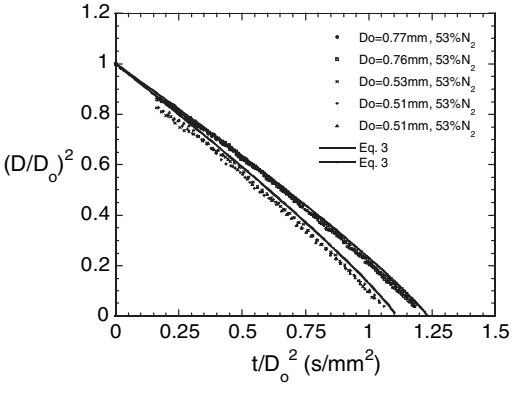

Fig. 7. Example illustrating Eq. (3) for predicting evolution of droplet diameter (data of Fig. 3c).

5. Conclusion

The burning process of nonane droplets with fixed oxygen and varying inert composition shows a strong initial droplet diameter dependence in a nitrogen inert that gradually decreases as nitrogen is diluted by helium. This trend indicates the diminished role of soot formation until with a oxygen/helium ambiance (no nitrogen present) there is virtually no dependence of burning rate on initial droplet diameter for droplets in the size range examined. The flame luminosity shows a progressive reduction with increasing helium concentration in the inert, and for an oxygen/helium gas the flame is entirely blue. This trend is consistent with the flame temperature decreasing as helium enriches the ambient gas. The time dependence of the burning rate is slight and it appears to have little to do with soot formation and more to do with progressive unsteadiness in the burning process that persists throughout the burning history even for the small droplet diameters examined here.

The burning rate depends on the initial droplet diameter in a nitrogen inert but not a helium inert. This fact shows the role of soot formation on altering the burning rate. For measurements scaled in the coordinates $(\frac{D}{D_o})^{2(1+\varepsilon)}$ and $\frac{t}{D_o^{2(1+\varepsilon)}}$, all the data for droplet diameter for a given gas composition are consolidated onto a single curve with the effective burning rate exhibiting virtually no dependence on initial droplet diameter and time.

Acknowledgments

The authors gratefully acknowledge the support of the National Aeronautics and Space Administration (NASA) through grant no. NAG-3-2224. The authors also wish to thank Dr. Daniel Dietrich of NASA for being the project monitor and Dr. Merrill King for being the Program Director.

References

[1] F.A. Williams, *Combustion Theory: The Fundamental Theory of Chemically Reacting Flow System*, second ed., The Benjamin/Cummings Publishing Company, Inc., Menlo Park, CA, (1985), p. 52–56, 64–65.
[2] G.A.E. Godsave, *Proc. Combust. Inst.* 4 (1953) 818–830.
[3] D.B. Spalding, *Proc. Combust. Inst.* 4 (1953) 847–864.
[4] G.S. Jackson, C.T. Avedisian, *Proc. R. Soc. Lond. A* 446 (1994) 255–276.

[5] A.J. Marchese, F.L. Dryer, R.O. Colantonio, *Proc. Combust. Inst.* 27 (1998) 2627–2634.
[6] O.L. Lee, S.L. Manzello, M.Y. Choi, *Comb. Sci. Technol.* 132 (1998) 139–156.
[7] G. Xu, M. Ikegami, S. Honma, K. Ikeda, X. Ma, H. Nagaishi, D.L. Dietrich, P.M. Struk, *Int. J. Heat Mass Trans.* 46 (2003) 1155–1169.
[8] J.H. Bae, *Experimental Observations and Analyses on the Dynamics of Isolated Spherical Droplet Flames Burning in Various Ambient Gases and Pressures*. Ph.D thesis, Sibley School of Mechanical and Aerospace Engineering, Cornell University (2005).
[9] C.T. Avedisian, B.J. Callahan, *Proc. Combust. Inst.* 28 (2000) 991–997.
[10] W. Tsang, Report No. NIST-IR-7155, National Institute of Standards and Technology, Gaithersburg, MD (2003).
[11] J.H. Bae, C.T. Avedisian, *Combust. Flame* 137 (2004) 148–162.
[12] C.T. Avedisian, *Physical and Chemical Aspects of Combustion (Chapter 6)*, Gordon and Breach Publ., Amsterdam, The Netherlands, 1997, p. 135–160.
[13] B.D. Shaw, F.A. Williams, *Int. J. Heat Mass Trans.* 33 (1990) 301–317.
[14] W.A. Sirignano, C.K. Law, *Adv. Chem. Ser.* 166 (1978) 3–26.
[15] G. Xu, M. Ikegami, S. Honma, M. Sasaki, K. Ikeda, H. Ngaishi, Y. Takeshita, *Fuel* 82 (2003) 319–330.
[16] M. Barrère, L. Nadaud, *Proc. Combust. Inst.* 10 (1965) 1381–1394.
[17] A.K. Ghosh, R. Natarajan, *Combust. Flame* 29 (1977) 283–287.
[18] I. Glassman, *Combustion*, third ed., Academic Press, San Diego, CA, 1996, p. 319.

Comments

Anthony J. Marchese, Rowan University, USA. You have shown that the burning rate of nonane decreases with increasing initial droplet diameter for conditions under which a soot shell is present. Do you believe that this phenomenon is a consequence of increased radiative heat loss with increasing initial droplet diameter?

Reply. We do believe that radiative losses are responsible for the slower burning of the larger droplets we examined relative to the smaller droplets in the cold ambience of our experiments. In a given inert, soot formation is influenced by the residence time of fuel molecules which in turn is proportional to the initial droplet diameter. Larger droplets tend to produce more soot with thicker shells for this reason. With larger droplets and more soot comes an increase of radiative losses which should slow the burning process as the initial droplet diameter increases, which is what we see in the data when nitrogen is present in the inert to produce a sooting nonane droplet flame. As the helium concentration in the inert is increased, however, less soot forms and the evolution of droplet diameter shows a progressively weaker influence of initial droplet diameter (in the coordinates of the "D^2" law). This effect seems to underscore the importance of luminous radiative losses since at the highest helium concentrations in the inert where the droplet flames are entirely blue, we observed no influence of initial droplet diameter on the burning rate. Only non-luminous radiative transport would be available to exert a radiation influence under those conditions, but apparently it does not for the small initial droplet diameters examined in this study.

•

Eva Gutheil, Heidelberg University, Germany. At this symposium, A. Yozgatligil et al. [1] also showed maximum soot formation for oxygen concentration of 30% for ethanol at elevated pressure. What is your motivation to study nonane as a fuel?

Reference

[1] A. Yozgatligil, S.-H. Park, M.Y. Choi, A. Kazakov, F.L. Dryer, *Proc. Combust. Inst.* 31 (2007), PROCI1158.

Reply. There are several reasons for examining nonane in our work. First, our study was performed at atmospheric pressure with a motivation to examine soot's role on the droplet burning process. A fuel which produces little or no soot at atmospheric pressure would therefore be no use to us for this purpose. Second, water is nearly insoluble in nonane whereas alcohols, especially methanol and to a lesser degree the higher alcohols including ethanol, have a higher propensity for water solubility by condensation on the droplet surface during burning than nonane. Water solubility is a complication we wished to avoid by selecting nonane in the interpretation of results. Third, as remarked in the presentation nonane is in a class of hydrocarbons (alkanes) which are currently being considered for inclusion in surrogate mixtures for complex transportation fuels (e.g., JP8), the idea being to select the surrogate chemical makeup and composition to match some particular combustion feature(s) of the real fuel to better allow the community to compare results and develop models for combustion. The spherical droplet flame is an attractive combustion configuration to accomplish this goal with its modelable (1D) transport configuration while also incorporating some of the unsteadiness inherent in the combustion of liquid fuels in practical devices.